

Nonreciprocal lensing and backscattering suppression via magneto-optical nonlocality

Dmitry Vagin¹ and Maxim A. Gorlach^{1,*}

¹*School of Physics and Engineering, ITMO University, Saint Petersburg 197101, Russia*

We introduce a special kind of nonreciprocal electromagnetic response which gives rise to backscattering suppression in the bulk, a long-sought feature in topological photonics, as well as nonreciprocal lensing – an effect when the same structure focuses light incident from one direction and defocuses light propagating in the opposite way. We predict this response in spin spirals and in specially designed metamaterials, validating the key predictions.

Introduction. – Artificial media have uncovered novel ways to manipulate the propagation of light via tailored electromagnetic responses [1–5]. When the period of the structure is much smaller than the wavelength, the composite can typically be viewed as a continuous medium possessing a set of frequency-dependent effective material parameters. In addition to the well-known permittivity and permeability those could include bianisotropy [6, 7] which results in the constitutive relations of the form

$$\mathbf{D} = \hat{\varepsilon} \mathbf{E} + (\hat{\chi} + i\hat{\kappa}) \mathbf{H}, \quad (1)$$

$$\mathbf{B} = (\hat{\chi} - i\hat{\kappa})^T \mathbf{E} + \hat{\mu} \mathbf{H}, \quad (2)$$

being a long-standing topic of active research [8, 9].

Even broader range of phenomena arises due to the electromagnetic nonlocality (spatial dispersion), when the effective permittivity of the medium depends not only on the frequency of the wave, but also on the wave vector [10]. This results in rich and diverse physics [11–14] which is a way more pronounced in metamaterials compared to the conventional media [9, 15].

On the other hand, the properties of the medium also depend on the applied static magnetic field giving rise to magneto-optical phenomena and electromagnetic nonreciprocity [16–18]. The latter ensures that the same medium transmits light differently in forward and backward direction providing a physical mechanism for optical isolation.

Interestingly, the interplay of nonlocal and nonreciprocal phenomena remains poorly studied. While the effects of magnetospatial dispersion are probed in condensed matter, their magnitude is very small [19–22]. In contrast, the metamaterial platform holds a promise to enhance these phenomena by orders of magnitude opening a door to the unique optical effects.

In this Letter, we reveal a special type of magneto-optical nonlocality which provides several important functionalities. First, it enables nonreciprocal lensing: focuses light propagating from one direction and defocuses light travelling in the opposite way. Second, the radiation pattern of any dipole source embedded in such medium is strongly non-symmetric thereby reducing backscattering on random defects in the entire bulk

of the medium. Below, we examine this physics, identifying the desired response in conical spin spirals and in a specially designed microwave metamaterial.

Symmetry analysis. – We describe the metamaterial in terms of the nonlocal permittivity tensor $\varepsilon_{ij}(\omega, \mathbf{k})$, where the dependencies on ω and \mathbf{k} capture the effects of frequency and spatial dispersion, respectively [16]. In addition, we assume a bias field $\mathbf{H}_0(\mathbf{r})$, odd under time reversal and responsible for nonreciprocity [17]. In the limit of weak spatial dispersion, we expand the permittivity as

$$\varepsilon_{ij}(\omega, \mathbf{k}) = \varepsilon_{ij}^{(e)}(\omega) + \varepsilon_{ij}^{(o)}(\omega) + \alpha_{ijl}^{(e)}(\omega) k_l + \alpha_{ijl}^{(o)}(\omega) k_l, \quad (3)$$

where the superscripts (e) and (o) denote even and odd components with respect to the reversal of the bias field $\mathbf{H}_0(\mathbf{r}) \rightarrow -\mathbf{H}_0(\mathbf{r})$. Assuming that the medium is lossless, we find $\varepsilon_{ij}(\omega, \mathbf{k}) = \varepsilon_{ji}^*(\omega, \mathbf{k})$ [16], and thus

$$\varepsilon_{ij}^{(e)} = \varepsilon_{ji}^{(e)*}, \quad \varepsilon_{ij}^{(o)} = \varepsilon_{ji}^{(o)*}, \quad (4)$$

$$\alpha_{ijl}^{(e)} = \alpha_{jil}^{(e)*}, \quad \alpha_{ijl}^{(o)} = \alpha_{jil}^{(o)*}. \quad (5)$$

On the other hand, the permittivity tensor is also constrained by Onsager-Kasimir relations [16, 17] $\varepsilon_{ij}(\omega, \mathbf{k}, \mathbf{H}_0) = \varepsilon_{ji}(\omega, -\mathbf{k}, -\mathbf{H}_0)$, which yields

$$\varepsilon_{ij}^{(e)} = \varepsilon_{ji}^{(e)}, \quad \varepsilon_{ij}^{(o)} = -\varepsilon_{ji}^{(o)}, \quad (6)$$

$$\alpha_{ijl}^{(e)} = -\alpha_{jil}^{(e)}, \quad \alpha_{ijl}^{(o)} = \alpha_{jil}^{(o)}. \quad (7)$$

Combining the conditions Eqs. (4)–(7), we recover that the tensor $\varepsilon_{ij}^{(e)}$ is real and symmetric, while $\varepsilon_{ij}^{(o)}$ is imaginary and antisymmetric. These tensors describe such well-known effects as anisotropy and magneto-optics [see Tab. I].

In the same spirit, we find out that the tensor $\alpha_{ijl}^{(e)}$ responsible for reciprocal nonlocality is imaginary and antisymmetric under the permutation of the first two indices. Tensor $\alpha_{ijl}^{(o)}$ captures magneto-optical nonlocality, being real and symmetric with respect to the same pair of indices. This response is odd both under spatial inversion \mathcal{P} and time reversal \mathcal{T} , being even under the combined \mathcal{PT} operation. In Table I we present the number of independent components for each of those tensors.

To connect α_{ijl} to the well-celebrated bianisotropy effects [7], we note that any bianisotropic medium with the permittivity $\hat{\varepsilon}$, chirality $\hat{\kappa}$ and Tellegen tensor $\hat{\chi}$ can

* m.gorlach@metalab.ifmo.ru

Contribution	Number of components	Physical phenomena
$\varepsilon_{ij}^{(e)}$	6	Anisotropy
$\varepsilon_{ij}^{(o)}$	3	Magneto-optics
$\alpha_{ijl}^{(e)}$	9	Electromagnetic chirality
$\alpha_{ijl}^{(o)}$	18	$\begin{cases} \text{Non-reciprocal bianisotropy (8)} \\ \text{Other phenomena (10)} \end{cases}$

TABLE I. Different contributions to the nonlocal permittivity tensor and underlying physical effects.

equivalently be described by the spatially dispersive permittivity [23]. Keeping the terms up to the first order in \mathbf{k} , we obtain:

$$\hat{\varepsilon}(\omega, \mathbf{k}) = \hat{\varepsilon} + \frac{i}{q} [\hat{\kappa} \mathbf{k}^\times + \mathbf{k}^\times \hat{\kappa}^T] + \frac{1}{q} [\hat{\chi} \mathbf{k}^\times - \mathbf{k}^\times \hat{\chi}^T]. \quad (8)$$

Here \mathbf{k}^\times is a matrix defined as $(\mathbf{k}^\times)_{ij} = -\epsilon_{ijl} k_l$, ϵ_{ijl} is the Levi-Civita symbol and $q = \omega/c$.

In bianisotropic framework, imaginary corrections linear in \mathbf{k} arise due to the chirality $\hat{\kappa}$. Since both κ_{ij} and $\alpha_{ijl}^{(e)}$ have 9 independent components, all reciprocal first-order spatial dispersion effects are perfectly captured by the chirality tensor [Table I].

At the same time, real corrections linear in \mathbf{k} are related to the Tellegen tensor $\hat{\chi}$. In addition, the component of $\hat{\chi}$ proportional to the identity matrix does not manifest itself in the bulk, reduces to the boundary term and captures axion electrodynamics [9, 24–28]. This leaves only 8 terms to capture magneto-optical nonlocality. However, the tensor $\alpha_{ijl}^{(o)}$ has 18 independent components and hence 10 of them are beyond bianisotropic framework Eq. (8). Those additional components are precisely the focus of our Letter.

Quasi-moving spatial dispersion. – Below, we focus on the specific type of magneto-optical nonlocality described by the tensor

$$\hat{\varepsilon}(\omega, \mathbf{k}) = \hat{\varepsilon}(\omega, 0) + \frac{\chi_{qm}}{q} \begin{pmatrix} 0 & 0 & k_x \\ 0 & 0 & k_y \\ k_x & k_y & 0 \end{pmatrix}, \quad (9)$$

where χ_{qm} is the dimensionless coefficient quantifying the strength of the effect. It is instructive to compare the form of the nonlocal contribution Eq. (9) to another celebrated nonreciprocal phenomenon – moving-type bianisotropy, which describes the propagation of light in a liquid moving with velocity $\mathbf{v} = (0, 0, v_z)^T$ relative to the laboratory frame. In the latter case, nonreciprocity tensor takes the form [23]

$$\hat{\chi} = \chi_m \begin{pmatrix} 0 & 1 & 0 \\ -1 & 0 & 0 \\ 0 & 0 & 0 \end{pmatrix}, \quad \chi_m = -\frac{v_z}{c}(\varepsilon - 1),$$

which can be recast as the nonlocal correction to the

permittivity tensor

$$\hat{\varepsilon}(\omega, \mathbf{k}) = \hat{\varepsilon}(\omega, 0) + \frac{\chi_m}{q} \begin{pmatrix} -2k_z & 0 & k_x \\ 0 & -2k_z & k_y \\ k_x & k_y & 0 \end{pmatrix}. \quad (10)$$

This suggests some parallels between the physics of the moving media and our nonlocal magneto-optical response which we further term “quasi-moving”.

A characteristic property of the moving medium is the Fresnel drag — the difference between the refractive indices of the wave propagating in forward and backward directions. Such difference is maximized when the wave vector is aligned with the velocity \mathbf{v} of the flow, and decreases to zero when $\mathbf{k} \perp \mathbf{v}$. This physics is readily visualized in terms of the isofrequency contours displaying the length of the wave vector k for various directions at a fixed frequency: the contours become shifted relative to the origin.

To probe related effects in our system, we solve the dispersion equation (see Supplementary Materials [29], Sec. I) and plot the family of isofrequency contours for the different strengths of χ_{qm} [Fig. 1(a)]. The contours exhibit a clear breaking of inversion symmetry, but in a peculiar manner. If the angle θ between the wave vector and Oz axis is equal to 0 or π , the nonreciprocal effect is hidden, and forward and backward-propagating waves have the same refractive index. However, the difference becomes noticeable at oblique incidence effectively featuring angle-dependent Fresnel drag.

Possible realization. – Importantly, the quasi-moving spatial dispersion occurs naturally and can be readily engineered in metamaterials without the need to modulate their parameters in time. This provides an advantage compared to the moving-type response, which was previously shown to occur in specially designed metasurfaces [8, 30, 31] or in the time-varying materials [32–34], which struggle to implement this physics in the visible range.

In contrast, the quasi-moving spatial dispersion is present even in the natural structures, where the combination of exchange and Dzyaloshinskii-Moriya interaction [35] enable helical arrangement of spins known as spin spiral [Fig. 1(b)]. We derive a simplified model capturing an effective response of such structures studying an idealized multilayered structure consisting of gyrotropic layers [29] (Sec. II), where the material equation for each layer reads

$$\mathbf{D} = \epsilon \mathbf{E} - i[\mathbf{g} \times \mathbf{E}], \quad (11)$$

and the component of gyrotropy vector \mathbf{g} tangential to the layer plane rotates from layer to layer. Assuming fixed angle β between the gyrotropy vector and the layer normal, we find

$$\chi_{qm} = \frac{q^3 g^3}{2b^3 \epsilon} \sin^2 \beta \cos \beta, \quad (12)$$

where the rotation rate of gyrotropy vector is assumed constant, and $b = 2\pi/a$ is reciprocal lattice constant. A

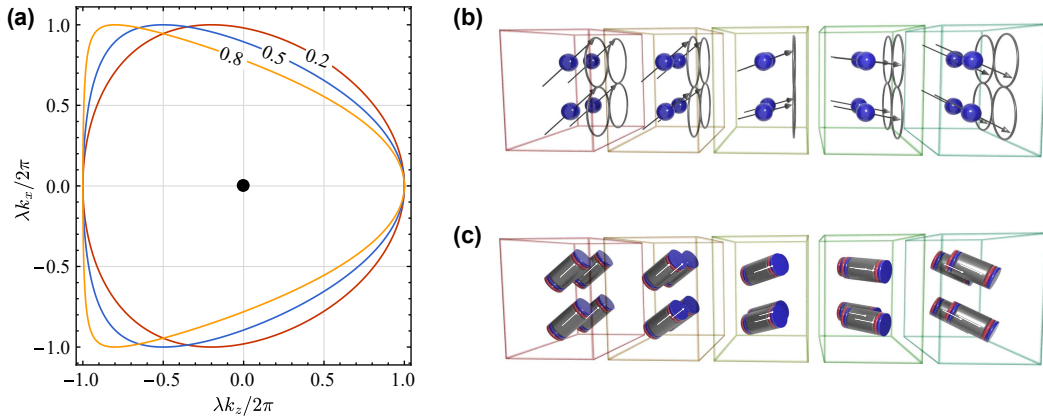


FIG. 1. (a) Isofrequency contours for the medium with quasi-moving spatial dispersion. Inversion symmetry of the contours is broken. Different colors encode the values of χ_{qm} labeled at the curves, λ denotes the wavelength in vacuum. For simplicity, we assume permittivity $\epsilon = 1$. (b) Spiral arrangement of spins in the lattice enabling quasi-moving spatial dispersion. (c) Metamaterial configuration producing enhanced quasi-moving response. Arrows indicate the direction of magnetization of the cylinders.

similar physics occurs if the gyrotropy of the permeability is considered instead:

$$\mathbf{B} = \mu \mathbf{H} - i[\mathbf{g} \times \mathbf{H}]. \quad (13)$$

The quasi-moving effect in such case reads

$$\chi_{qm} = -\frac{q^3 g^3}{2b^3 \mu} \sin^2 \beta \cos \beta. \quad (14)$$

We anticipate that the quasi-moving spatial dispersion naturally occurs in chiral magnets [36], including conical spin-spirals [37]. Qualitatively, these structures may be approximately described by the simplified model of gyrotropic layers when the wavelength exceeds the lattice constant multiple times. A promising candidate for such physics in the optical range is bismuth ferrite (BiFeO_3). This compound has spiral magnetic ordering [38], is transparent for visible light [39] and possesses significant anisotropy [40].

On the other hand, the strength of the quasi-moving effect at microwave frequencies can be strongly amplified by harnessing microwave metamaterials and magnetized yttrium iron garnet (YIG) cylinders [see Fig. 1(c)], which previously proved to be instrumental in probing photonic topological phenomena [41] or realizing strong Tellegen response [9]. In such case, the gyrotropy of YIG cylinders can reach the values up to $g \approx 1.5$ at resonance, which allows us to estimate attainable quasi-moving effect as $\chi_{qm} \approx 0.2$ [29] (Sec. III). Our estimates thus suggest that the quasi-moving spatial dispersion is achievable and sizable in realistic materials. We now proceed to studying optical phenomena it unlocks.

Non-reciprocal lens. – Nonreciprocal nature of the material opens a possibility to construct a lens that has different focal distances for the two opposite directions of light propagation along the z axis. For instance, this sys-

tem could focus light incident from the left and defocus rays coming from the right [Fig. 2(a)].

To evaluate the focal distance of a thin lens, we employ the paraxial approximation $|k_x/k_z| \ll 1$. For a substantial range of angles it is reasonable to terminate the expansion of the even function $n(k_x)$ derived from the dispersion equation on the quadratic contribution

$$n(k_x) = n_{\parallel} + \zeta \frac{k_x^2}{k^2} = n_{\parallel} + \zeta \sin^2 \theta, \quad (15)$$

where coefficients n_{\parallel} and ζ are the material characteristics, and θ is the angle between the wave vector and the optical axis. For quasi-moving medium we obtain

$$\zeta = -\frac{\chi_{qm}}{q^2 \epsilon} - \frac{\chi_{qm}^2}{2q \epsilon^{3/2}}. \quad (16)$$

The dependence of effective refractive index on the angle θ modifies the optical paths for the rays traversing the system and hence affects the location of the focal spot. Since χ_{qm} is inversion-odd, the ζ term has different values for the light propagating in forward and backward directions. This opens a prospect of non-reciprocal lensing.

Expanding the expression for the optical path length and keeping the terms up to θ^2 , we recover a thin lens formula [29] (Sec. IV) $1/F = 1/d_o + 1/d_i$, where d_o and d_i denote distances from the lens to an object and its image, respectively. However, the expression for the optical power is modified:

$$\frac{1}{F} = \frac{n_{2\parallel} - n_{1\parallel}}{n_{1\parallel} + 2\zeta_1} \left(\frac{1}{R_1} - \frac{1}{R_2} \right).$$

Here R_1 and R_2 are curvature radii of the refractive surfaces, $n_{1\parallel}$ and ζ_1 are the properties of the medium surrounding the lens, while $n_{2\parallel}$ corresponds to the lens itself.

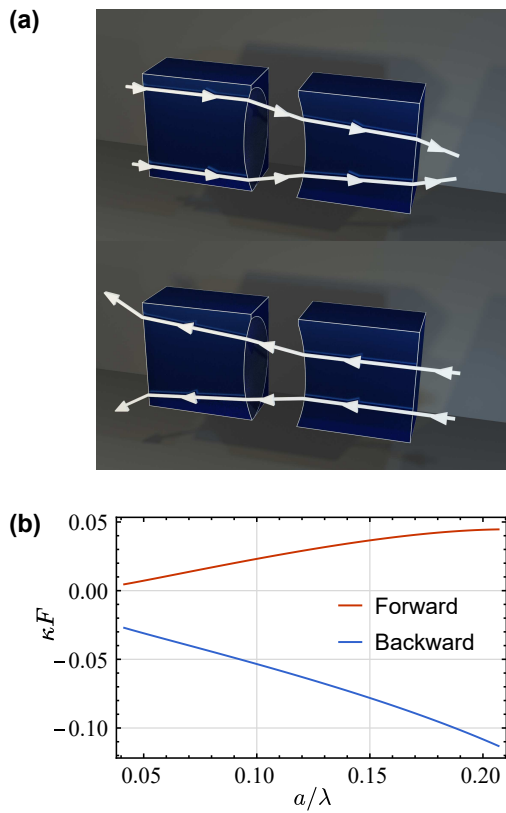


FIG. 2. (a) Artistic image of a non-reciprocal lens, with light paths traced for left-to-right and right-to-left propagation. (b) Focal distance for the fixed light polarization computed for two opposite propagation directions. Material characteristics $\varepsilon_{\perp} = 2.9$, $\varepsilon_{\parallel} = 1.0$, $N = 30$, $g = 0.9$, $\beta = 0.3\pi$. The focal distance is multiplied by the combined curvature $\kappa = 1/R_1 - 1/R_2$ of the refractive surfaces.

The result does not depend on ζ_2 . Hence, a promising configuration is a lens-shaped cavity cut into two slabs of the quasi-moving material, Fig. 2(a).

By the proper choice of parameters, we ensure that this lens can focus and defocus light depending on the direction it propagates. In Figure 2(b) we plot the focal distances, corresponding to the fixed light polarization: right circular polarization in the case of normal incidence and its continuous modification for oblique incidence. The focal distances for the two illumination directions are profoundly different and even have different signs. A similar physics occurs for another polarization with less pronounced nonreciprocal effect and the same sign of the focal distances for both propagation directions. An additional property of this system is particularly small focal length per given curvature. This contrasts with the performance of the lenses made from isotropic materials with positive refractive index, where the quantity κF is always larger than 1.

Backscattering suppression. – Yet another application of the quasi-moving effect is the control of the radia-

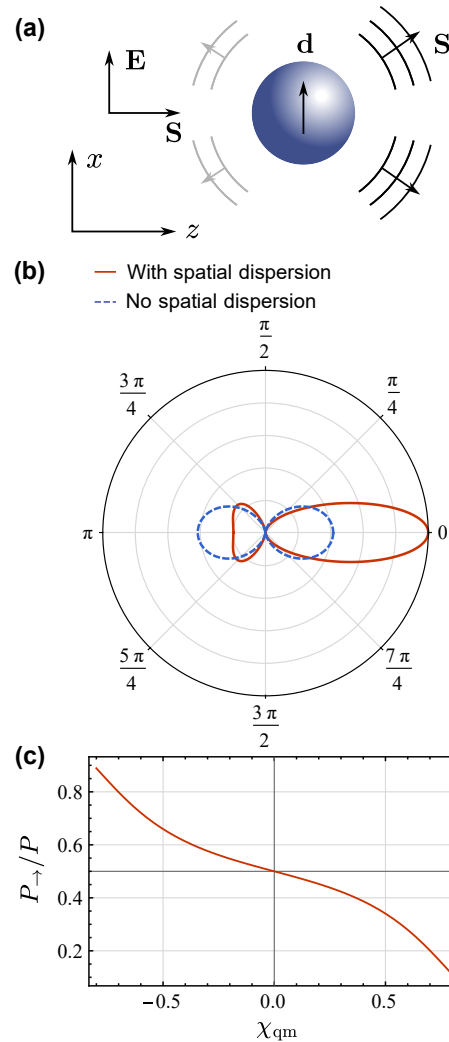


FIG. 3. Asymmetric scattering in the quasi-moving medium: (a) A schematic image of a random defect excited by an electromagnetic wave and radiating mostly forward. (b) Radiation pattern for the x -aligned dipole in quasi-moving medium with $\chi_{qm} = -0.2$ shown in Oxz plane. (c) The ratio of power radiated in the forward $+z$ direction to the total radiation power versus the strength of the quasi-moving effect χ_{qm} .

tion power distribution. The far-field analysis based on the Fourier transformation and stationary phase approximation demonstrates [29] (Sec. V) that an oscillating dipole radiates asymmetrically in the quasi-moving environment, Fig. 3(a). The typical radiation pattern of a dipole oscillating in the direction orthogonal to the spin spiral axis calculated for the case of microwave metamaterial is presented in Fig. 3(b). To quantify the asymmetry of the radiation pattern, we calculate the ratio between the power radiated to the semi-space $z > 0$ P_{\rightarrow} and the total scattered power P in Fig. 3(c). In particular, experimentally achievable value $\chi_{qm} \approx -0.2$ leads to the ratio around 0.55; stronger asymmetry is available in photonic crystal regime. Notably, asymmetry in the

radiation pattern persists for other dipole alignments as well [29] (Sec. V).

Hence, if the wave propagating in the quasi-moving material in $+z$ direction encounters a defect, only a minor part of the wave energy will be backscattered. Notably, such partial backscattering immunity is guaranteed in the entire bulk of the material. This contrasts with the behavior of topological materials, where backscattering immunity is stronger, but occurs only in a small spatial region occupied by the topological edge modes.

In summary, we have shown that the interplay of nonlocality and magneto-optical nonreciprocity enables a plethora of exciting optical phenomena which include nonreciprocal lensing and backscattering suppression in the bulk of the medium. This rich physics is beyond the bianisotropic framework and until now remained vastly

unexplored. At the same time, the associated phenomena are well within the reach of modern experiments and arise not only in a class of magnetic materials in condensed matter, but also can be tailored in the microwave metamaterials, where magneto-optical nonreciprocal effects can be enhanced by orders of magnitude, which promises fruitful applications in nonreciprocal routing of light and topological photonics.

ACKNOWLEDGMENTS

This work was supported by the Russian Science Foundation grant No. 25-79-31027.

[1] V. G. Veselago, The electrodynamics of substances with simultaneously negative values of ϵ and μ , Soviet Physics Uspekhi **10**, 509 (1968).

[2] G. V. Eleftheriades and K. G. Balmain, *Negative-Refraction Metamaterials: Fundamental Principles and Applications* (Wiley, Hoboken, NJ, 2005).

[3] T. Itoh and C. Caloz, *Electromagnetic Metamaterials: Transmission Line Theory and Microwave Applications* (Wiley, Hoboken, NJ, 2005).

[4] R. Marques, F. Martin, and M. Sorolla, *Metamaterials with Negative Parameters* (Wiley, Hoboken, NJ, 2008).

[5] F. Capolino, ed., *Theory and Phenomena of Metamaterials* (CRC Press, New York, 2009).

[6] J. A. Kong, Optics of bianisotropic media, Journal of the Optical Society of America **64**, 1304 (1974).

[7] A. Serdyukov, I. Semchenko, S. Tretyakov, and A. Sihvola, *Electromagnetics of Bi-anisotropic Materials: Theory and Applications* (Gordon and Breach Science, Amsterdam, 2001).

[8] V. S. Asadchy, A. Díaz-Rubio, and S. A. Tretyakov, Bianisotropic metasurfaces: physics and applications, Nanophotonics **7**, 1069 (2018).

[9] Q. Yang, X. Wen, Z. Li, O. You, and S. Zhang, Gigantic Tellegen responses in metamaterials, Nature Communications **16**, 151 (2025).

[10] V. M. Agranovich and V. Ginzburg, *Crystal Optics with Spatial Dispersion, and Excitons* (Springer Berlin Heidelberg, 1984).

[11] P. A. Belov, R. Marqués, S. I. Maslovski, I. S. Nefedov, M. Silveirinha, C. R. Simovski, and S. A. Tretyakov, Strong spatial dispersion in wire media in the very large wavelength limit, Physical Review B **67**, 113103 (2003).

[12] A. Silva, F. Monticone, G. Castaldi, V. Galdi, A. Alù, and N. Engheta, Performing Mathematical Operations with Metamaterials, Science **343**, 160 (2014).

[13] J. Luo, Y. Yang, Z. Yao, W. Lu, B. Hou, Z. H. Hang, C. Chan, and Y. Lai, Ultratransparent Media and Transformation Optics with Shifted Spatial Dispersions, Physical Review Letters **117**, 223901 (2016).

[14] K. Shastri and F. Monticone, Nonlocal flat optics, Nature Photonics **17**, 36 (2022).

[15] M. A. Gorlach, S. B. Glybovski, A. A. Hurshkainen, and P. A. Belov, Giant spatial-dispersion-induced birefringence in metamaterials, Physical Review B **93**, 201115 (2016).

[16] L. Landau and E. Lifshitz, *Electrodynamics of Continuous Media* (Pergamon Press, Oxford, 1984).

[17] C. Caloz, A. Alù, S. Tretyakov, D. Sounas, K. Achouri, and Z.-L. Deck-Léger, Electromagnetic nonreciprocity, Physical Review Applied **10**, 047001 (2018).

[18] V. S. Asadchy, M. S. Mirmoosa, A. Díaz-Rubio, S. Fan, and S. A. Tretyakov, Tutorial on Electromagnetic Nonreciprocity and its Origins, Proceedings of the IEEE **108**, 1684 (2020).

[19] D. Portigal and E. Burstein, Magneto-spatial dispersion effects on the propagation of electro-magnetic radiation in crystals, Journal of Physics and Chemistry of Solids **32**, 603 (1971).

[20] E. L. Ivchenko, V. P. Kochereshko, G. V. Mikhailov, and I. N. Uraltsev, Resonance Magneto-Spatial Dispersion of Crystals, Physica Status Solidi B **122**, 221 (1984).

[21] B. B. Krichevskov, R. V. Pisarev, A. A. Rzhevsky, V. N. Gridnev, and H.-J. Weber, Magnetospatial dispersion effect in magnetic semiconductors $Cd_{1-x}Mn_xTe$, Physical Review B **57**, 14611 (1998).

[22] L. V. Kotova, V. N. Kats, A. V. Platonov, V. P. Kochereshko, R. André, and L. E. Golub, Magnetospatial dispersion of semiconductor quantum wells, Physical Review B **97**, 125302 (2018).

[23] J. A. Kong, *Electromagnetic wave theory* (Wiley, 1990).

[24] F. Wilczek, Two applications of axion electrodynamics, Physical Review Letters **58**, 1799 (1987).

[25] D. M. Nenno, C. A. C. Garcia, J. Gooth, C. Felser, and P. Narang, Axion physics in condensed-matter systems, Nature Reviews Physics **2**, 682 (2020).

[26] L. Shaposhnikov, M. Mazanov, D. A. Bobylev, F. Wilczek, and M. A. Gorlach, Emergent axion response in multilayered metamaterials, Physical Review B **108**, 115101 (2023).

[27] S. Safaei Jazi, I. Faniaye, R. Cicheler, D. C. Tzarouchis, M. M. Asgari, A. Dmitriev, S. Fan, and V. Asadchy, Optical Tellegen metamaterial with spontaneous magnetization, Nature Communications **15**, 1293 (2024).

[28] G.-G. Liu, S. Mandal, X. Xi, Q. Wang, C. Devescovi, A. Morales-Pérez, Z. Wang, L. Yang, R. Banerjee, Y. Long, Y. Meng, P. Zhou, Z. Gao, Y. Chong, A. García-Etxarri, M. G. Vergniory, and B. Zhang, Photonic axion insulator, *Science* **387**, 162 (2025).

[29] See Supplementary Materials for the derivation of effective material parameters of conical spin spirals, evaluation of the possible quasi-moving effect in a microwave metamaterial, calculation of a focal length of a thin lens in a quasi-moving medium and computation of the dipole radiation pattern in such material, which includes Refs. [16, 41].

[30] Y. Ra'di and A. Grbic, Magnet-free nonreciprocal bianisotropic metasurfaces, *Physical Review B* **94**, 195432 (2016).

[31] T. Kodama, T. Nakanishi, K. Sawada, and S. Tomita, Pure moving optical media consisting of magnetochiral metasurfaces, *Optical Materials Express* **14**, 2499 (2024).

[32] D.-W. Wang, H.-T. Zhou, M.-J. Guo, J.-X. Zhang, J. Evers, and S.-Y. Zhu, Optical diode made from a moving photonic crystal, *Physical Review Letters* **110**, 093901 (2013).

[33] P. A. Huidobro, E. Galiffi, S. Guenneau, R. V. Craster, and J. B. Pendry, Fresnel drag in space-time-modulated metamaterials, *Proceedings of the National Academy of Sciences* **116**, 24943 (2019).

[34] E. Galiffi, R. Tirole, S. Yin, H. Li, S. Vezzoli, P. A. Huidobro, M. G. Silveirinha, R. Sapienza, A. Alù, and J. B. Pendry, Photonics of time-varying media, *Advanced Photonics* **4**, 014002 (2022).

[35] M. Cherkasskii, R. Mondal, and L. Rózsa, Inertial spin waves in spin spirals, *Physical Review B* **109**, 184424 (2024).

[36] Y. Togawa, Y. Kousaka, K. Inoue, and J.-i. Kishine, Symmetry, structure, and dynamics of monoaxial chiral magnets, *Journal of the Physical Society of Japan* **85**, 112001 (2016).

[37] D. Wuhrer, L. Rózsa, U. Nowak, and W. Belzig, Magnon squeezing in conical spin spirals, *Physical Review Research* **5**, 043124 (2023).

[38] I. Sosnowska, T. P. Neumaier, and E. Steichele, Spiral magnetic ordering in bismuth ferrite, *Journal of Physics C: Solid State Physics* **15**, 4835 (1982).

[39] A. Kumar, R. C. Rai, N. J. Podraza, S. Denev, M. Ramirez, Y.-H. Chu, L. W. Martin, J. Ihlefeld, T. Heeg, J. Schubert, D. G. Schlom, J. Orenstein, R. Ramesh, R. W. Collins, J. L. Musfeldt, and V. Gopalan, Linear and nonlinear optical properties of BiFeO_3 , *Applied Physics Letters* **92**, 121915 (2008).

[40] J.-P. Rivera and H. Schmid, On the birefringence of magnetoelectric BiFeO_3 , *Ferroelectrics* **204**, 23 (1997).

[41] P. Zhou, G.-G. Liu, Y. Yang, Y.-H. Hu, S. Ma, H. Xue, Q. Wang, L. Deng, and B. Zhang, Observation of Photonic Antichiral Edge States, *Physical Review Letters* **125**, 263603 (2020).

**Supplementary Materials:
Nonreciprocal lensing and backscattering suppression via magneto-optical nonlocality**

Dmitry Vagin¹ and Maxim A. Gorlach^{1,*}

¹*School of Physics and Engineering, ITMO University, Saint Petersburg 197101, Russia*

CONTENTS

I. Dispersion equation and eigenmodes in quasi-moving medium	1
II. Effective medium treatment of conical spin spirals	2
III. Estimates of the quasi-moving effect in microwave metamaterials	6
IV. Focal length of a lens in a quasi-moving medium	6
V. Dipole radiation in a quasi-moving medium	7
References	10

I. DISPERSION EQUATION AND EIGENMODES IN QUASI-MOVING MEDIUM

Refractive indices and polarizations of the eigenmodes in the medium are essential in the analysis of light propagation. Here we examine the case of quasi-moving nonreciprocal medium. We start from the equation for the electric field of the eigenmode [1]

$$(\mathbf{k} \otimes \mathbf{k} - k^2 \hat{1} - q^2 \varepsilon(\omega, k)) \mathbf{E} = 0.$$

Using the expression for the nonlocal permittivity of the quasi-moving medium and setting $k_y = 0$, which is possible due to the rotational symmetry around the axis z , we obtain

$$\begin{pmatrix} k_z^2 - q^2 \varepsilon & 0 & -q\chi_{qm} k_x - k_z k_x \\ 0 & k_x^2 + k_z^2 - q^2 \varepsilon & 0 \\ -q\chi_{qm} k_x - k_z k_x & 0 & k_x^2 - q^2 \varepsilon \end{pmatrix} \mathbf{E} = 0$$

The eigenmode structure is largely similar to the modes of a uniaxial crystal: there is a TE mode, with $E_x = E_z = 0$, $E_y \neq 0$, and TM mode polarized in the (xz) plane. The TE mode does not acquire nonreciprocal contribution, its refractive index $n = \sqrt{\varepsilon}$. The TM mode dispersion is found by equating the determinant of the given matrix to zero, which yields the solutions

$$k_z = \pm \frac{\sqrt{(k_x^2 - q^2 \varepsilon)(\chi_{qm}^2 k_x^2 - q^2 \varepsilon^2)}}{q\varepsilon} - \frac{\chi_{qm} k_x^2}{q\varepsilon}. \quad (S1)$$

Notably, the magnitude of k_z for the opposite propagation directions is different which is due to the nonreciprocal term χ_{qm} . Interestingly, the asymmetry disappears under the normal incidence when $k_x = 0$.

Note that these equations apply to a ‘pure’ quasi-moving effect, without any additional spatially dispersive terms or anisotropic contributions. Thus, they do not describe a gyrotropic metamaterial presented further, which, aside from nonreciprocal spatial dispersion, features pronounced magneto-optical and chiral effects. Those lead to the circular polarization of the eigenmodes at normal incidence ($k_x = 0$) and near-circular polarization at oblique incidence.

* m.gorlach@metalab.ifmo.ru

II. EFFECTIVE MEDIUM TREATMENT OF CONICAL SPIN SPIRALS

In this section we show how the quasi-moving spatial dispersion arises in a simplified model of a conical spin spiral. While the rigorous analysis requires quantum-mechanical description of interactions between the spins in the lattice, here we utilize a classical model which embodies all underlying symmetries of a solid state structure and provides conceptually clear picture.

In this description, the spins or meta-atoms are replaced by layered structure with the constant magnetization in each layer. The magnetization generates a gyrotropic term in the constitutive relations:

$$\mathbf{D} = \mathbf{E} - i[\mathbf{g} \times \mathbf{E}] \quad (\text{S2})$$

Here \mathbf{g} is parallel to the magnetization, i.e. spins. As we are studying the case of spin spiral, the direction of \mathbf{g} periodically depends on the coordinate z :

$$\mathbf{g} = g \begin{pmatrix} \sin \beta \sin \frac{2\pi z}{a} \\ \sin \beta \cos \frac{2\pi z}{a} \\ \cos \beta \end{pmatrix} = \begin{pmatrix} g_{\perp} \sin \frac{2\pi z}{a} \\ g_{\perp} \cos \frac{2\pi z}{a} \\ g_z \end{pmatrix}$$

where β is the cone angle and a is the period of spin spiral. As the spins are localized in the sites of the lattice, the actual magnetization is non-uniform. Here, for simplicity, we assume that the vector \mathbf{g} is uniform in the Oxy plane.

As a result, the problem reduces to investigating the solutions of Maxwell's equations in a planar geometry where the gyrotropy axis rotates with the z coordinate. Due to the translational symmetry of this structure, we can apply Bloch theorem and expand the field as:

$$\begin{pmatrix} \mathbf{E}(\mathbf{r}) \\ \mathbf{B}(\mathbf{r}) \\ \mathbf{D}(\mathbf{r}) \\ \mathbf{H}(\mathbf{r}) \end{pmatrix} = \sum_{n=-\infty}^{\infty} \begin{pmatrix} \mathbf{E}_n \\ \mathbf{B}_n \\ \mathbf{D}_n \\ \mathbf{H}_n \end{pmatrix} e^{i\mathbf{k}_n \cdot \mathbf{r} - \xi i q c t},$$

where

$$\mathbf{k}_n = \xi \mathbf{k} + n \mathbf{b}, \quad \mathbf{b} = \frac{2\pi}{a} \mathbf{e}_z, \quad q = \frac{\omega}{c}$$

In our effective medium analysis we assume that wavelength is much larger then the period of the structure which leads to the conditions $k \ll b$ and $q \ll b$. Next we introduce a dimensionless parameter ξ , which controls the wavelength scale, and explore the series expansion of the solution near $\xi = 0$. The substitution of Floquet harmonics allows us to recast Maxwell's equation in the form

$$\begin{cases} n \mathbf{b} \times \mathbf{H}_n = \xi(-\mathbf{k} \times \mathbf{H}_n - q \mathbf{D}_n) + \frac{4\pi}{ic} \mathbf{j} \delta_{n,0} \\ n \mathbf{b} \cdot \mathbf{D}_n = \xi(-\mathbf{k} \cdot \mathbf{D}_n) + \frac{4\pi}{i} \rho \delta_{n,0} \\ n \mathbf{b} \times \mathbf{E}_n = \xi(-\mathbf{k} \times \mathbf{E}_n + q \mathbf{B}_n) \\ n \mathbf{b} \cdot \mathbf{B}_n = \xi(-\mathbf{k} \cdot \mathbf{B}_n). \end{cases} \quad (\text{S3})$$

These equations can be rewritten compactly by utilizing a specific grouping of the fields:

$$\begin{aligned} \mathbf{F} &= (E_x, E_y, D_z, H_x, H_y, B_z)^T \\ \mathbf{G} &= (D_x, D_y, E_z, B_x, B_y, H_z)^T \end{aligned}$$

By using this substitution we reduce Eq. (S3) to a single matrix equation

$$\mathbf{F}_n = \frac{\xi}{bn} (-k_z \mathbf{F}_n + \hat{\eta} \mathbf{G}_n), \quad n \neq 0, \quad (\text{S4})$$

where

$$\hat{\eta} = \begin{pmatrix} 0 & 0 & k_1 & 0 & q & 0 \\ 0 & 0 & k_2 & -q & 0 & 0 \\ -k_1 & -k_2 & 0 & 0 & 0 & 0 \\ 0 & -q & 0 & 0 & 0 & k_1 \\ q & 0 & 0 & 0 & 0 & k_2 \\ 0 & 0 & 0 & -k_1 & -k_2 & 0 \end{pmatrix} = \begin{pmatrix} [\mathbf{e}_z^\times, \mathbf{k}^\times] & -q\mathbf{e}_z^\times \\ q\mathbf{e}_z^\times & [\mathbf{e}_z^\times, \mathbf{k}^\times] \end{pmatrix}.$$

The series expansion near $\xi = 0$ reads

$$\mathbf{F}_n = \sum_{\mu=0}^{\infty} \xi^{\mu} \mathbf{F}_n^{(\mu)}, \quad \mathbf{G}_n = \sum_{\mu=0}^{\infty} \xi^{\mu} \mathbf{G}_n^{(\mu)}. \quad (\text{S5})$$

Thus, the relation S4 can be used to express the next order using the previous one:

$$\mathbf{F}_n^{(\mu+1)} = \frac{1}{bn} \left(-k_z \mathbf{F}_n^{(\mu)} + \hat{\eta} \mathbf{G}_n^{(\mu)} \right), \quad n \neq 0. \quad (\text{S6})$$

Constitutive relations can be expressed via \mathbf{F} and \mathbf{G} as well. Due to linearity of the constitutive relations, there exists a matrix $\hat{\iota}$ satisfying $\mathbf{G} = \hat{\iota} \mathbf{F}$. By applying this relation to the Floquet harmonics we find

$$\mathbf{G}_n = \sum_{n'} \hat{\iota}_{n-n'} \mathbf{F}_{n'}, \quad (\text{S7})$$

where $\hat{\iota}_n$ are Fourier coefficients of $\hat{\iota}$,

$$\hat{\iota}(z) = \sum_n \hat{\iota}_n e^{inbz}$$

Note that the equations for $n = 0$ need not be solved for the derivation of effective response, as it is sufficient to find all fields as functions of \mathbf{F}_0 . Constitutive relations and Maxwell's equations are linear, so we expect the linear mapping given by matrices \hat{F}_n^μ and \hat{G}_n^μ :

$$\mathbf{F}_n^{(\mu)} = \hat{F}_n^{(\mu)} \mathbf{F}_0, \quad \mathbf{G}_n^{(\mu)} = \hat{G}_n^{(\mu)} \mathbf{F}_0. \quad (\text{S8})$$

The assumption of constant \mathbf{F}_0 , together with Maxwell's equations (S6) and constitutive relations (S7) generate a system of recurrence relations:

$$\begin{cases} \hat{F}_n^{(\mu+1)} = \frac{1}{bn} (-k_z \hat{F}_n^{(\mu)} + \hat{\eta} \hat{G}_n^{(\mu)}), & n \neq 0 \\ \hat{F}_0^{(\mu+1)} = 0 \\ \hat{G}_n^{(\mu+1)} = \sum_{n'} \hat{\iota}_{n-n'} \hat{F}_n^{(\mu+1)} \end{cases} \quad (\text{S9})$$

In the case of material equations with rotating gyrotropy, Eq. (S2), the matrix $\hat{\iota}$ reads

$$\hat{\iota}(z) = \begin{pmatrix} \varepsilon - \frac{\sin^2(\frac{2\pi z}{a})g_{\perp}^2}{\varepsilon} & \frac{\sin(\frac{4\pi z}{a})g_{\perp}^2}{2\varepsilon} + ig_z & -\frac{i\sin(\frac{2\pi z}{a})g_{\perp}}{\varepsilon} & 0 & 0 & 0 \\ \frac{\sin(\frac{4\pi z}{a})g_{\perp}^2}{2\varepsilon} - ig_z & \varepsilon - \frac{\cos^2(\frac{2\pi z}{a})g_{\perp}^2}{\varepsilon} & \frac{i\cos(\frac{2\pi z}{a})g_{\perp}}{\varepsilon} & 0 & 0 & 0 \\ -\frac{i\sin(\frac{2\pi z}{a})g_{\perp}}{\varepsilon} & \frac{i\cos(\frac{2\pi z}{a})g_{\perp}}{\varepsilon} & \frac{1}{\varepsilon} & 0 & 0 & 0 \\ 0 & 0 & 0 & 1 & 0 & 0 \\ 0 & 0 & 0 & 0 & 1 & 0 \\ 0 & 0 & 0 & 0 & 0 & 1 \end{pmatrix}$$

Using recurrence relations (S9) the following contributions to \hat{G}_0 are evaluated (for brevity we omit the terms quadratic in \mathbf{k}):

$$\begin{aligned}\hat{G}_0^{(0)} &= \begin{pmatrix} \varepsilon - \frac{g_\perp^2}{2\varepsilon} & ig_z & 0 & 0 & 0 & 0 \\ -ig_z & \varepsilon - \frac{g_\perp^2}{2\varepsilon} & 0 & 0 & 0 & 0 \\ 0 & 0 & \frac{1}{\varepsilon} & 0 & 0 & 0 \\ 0 & 0 & 0 & 1 & 0 & 0 \\ 0 & 0 & 0 & 0 & 1 & 0 \\ 0 & 0 & 0 & 0 & 0 & 1 \end{pmatrix}, \\ \hat{G}_0^{(1)} &= \begin{pmatrix} 0 & 0 & -\frac{ig_\perp^2 k_y}{2b\varepsilon^2} & 0 & 0 & 0 \\ 0 & 0 & \frac{ig_\perp^2 k_x}{2b\varepsilon^2} & 0 & 0 & 0 \\ -\frac{ig_\perp^2 k_y}{2b\varepsilon^2} & \frac{ig_\perp^2 k_x}{2b\varepsilon^2} & 0 & 0 & 0 & 0 \\ 0 & 0 & 0 & 0 & 0 & 0 \\ 0 & 0 & 0 & 0 & 0 & 0 \\ 0 & 0 & 0 & 0 & 0 & 0 \end{pmatrix}, \\ \hat{G}_0^{(2)} &= \begin{pmatrix} \frac{q^2 g_\perp^4}{16b^2 \varepsilon^2} & 0 & 0 & 0 & 0 & 0 \\ 0 & \frac{q^2 g_\perp^4}{16b^2 \varepsilon^2} & 0 & 0 & 0 & 0 \\ 0 & 0 & -\frac{q^2 g_\perp^2}{b^2 \varepsilon^2} & 0 & 0 & 0 \\ 0 & 0 & 0 & 0 & 0 & 0 \\ 0 & 0 & 0 & 0 & 0 & 0 \\ 0 & 0 & 0 & 0 & 0 & 0 \end{pmatrix}, \\ \hat{G}_0^{(3)} &= \begin{pmatrix} 0 & \frac{iq^2 g_\perp^4 k_z}{16b^3 \varepsilon^2} & \frac{q^2 g_\perp^2 (8\varepsilon g_z k_x - i(8\varepsilon^2 - 9g_\perp^2)k_y)}{16b^3 \varepsilon^3} & 0 & 0 & 0 \\ -\frac{iq^2 g_\perp^4 k_z}{16b^3 \varepsilon^2} & 0 & \frac{q^2 g_\perp^2 (i(8\varepsilon^2 - 9g_\perp^2)k_x + 8\varepsilon g_z k_y)}{16b^3 \varepsilon^3} & 0 & 0 & 0 \\ \frac{iq^2 g_\perp^2 (8i\varepsilon g_z k_x + (9g_\perp^2 - 8\varepsilon^2)k_y)}{16b^3 \varepsilon^3} & \frac{iq^2 g_\perp^2 ((8\varepsilon^2 - 9g_\perp^2)k_x + 8i\varepsilon g_z k_y)}{16b^3 \varepsilon^3} & 0 & 0 & 0 & 0 \\ 0 & 0 & 0 & 0 & 0 & 0 \\ 0 & 0 & 0 & 0 & 0 & 0 \\ 0 & 0 & 0 & 0 & 0 & 0 \end{pmatrix}.\end{aligned}$$

From these expressions we immediately find the effective parameters: since $\mathbf{G}_0^{(\mu)} = \hat{G}_0^{(\mu)} \mathbf{F}_0$, the effective response, connecting 0-th Floquet harmonics, becomes apparent.

$$\mathbf{G}_0 = \hat{\iota}_{\text{eff}} \mathbf{F}_0 = \sum_{\mu=0}^{\infty} \xi^{\mu} \hat{G}_0^{(\mu)} \mathbf{F}_0, \quad \hat{\iota}_{\text{eff}} = \sum_{\mu=0}^{\infty} \xi^{\mu} \hat{G}_0^{(\mu)} \quad (\text{S10})$$

We observe that $\hat{\iota}$ has the following block form:

$$\hat{\iota}_{\text{eff}} = \begin{pmatrix} \hat{\sigma} & 0 \\ 0 & 1 \end{pmatrix},$$

which corresponds to magnetic permeability $\hat{\mu}_{\text{eff}} = 1$ and permittivity

$$\hat{\varepsilon}_{\text{eff}} = \begin{pmatrix} \sigma_{xx} - \frac{\sigma_{xz}\sigma_{zx}}{\sigma_{zz}} & \sigma_{xy} - \frac{\sigma_{xz}\sigma_{zy}}{\sigma_{zz}} & \frac{\sigma_{xz}}{\sigma_{zz}} \\ \sigma_{yx} - \frac{\sigma_{yz}\sigma_{zx}}{\sigma_{zz}} & \sigma_{yy} - \frac{\sigma_{yz}\sigma_{zy}}{\sigma_{zz}} & \frac{\sigma_{yz}}{\sigma_{zz}} \\ -\frac{\sigma_{zx}}{\sigma_{zz}} & -\frac{\sigma_{zy}}{\sigma_{zz}} & \frac{1}{\sigma_{zz}} \end{pmatrix}.$$

After explicit evaluation of $\hat{\varepsilon}_{\text{eff}}$, we separate it into three components: constant anisotropic and magneto-optic terms, spatially dispersive chiral term and non-reciprocal quasi-moving element:

$$\hat{\varepsilon}_{\text{eff}} = \hat{\varepsilon}_{\text{const}} + \hat{\varepsilon}_{\text{chiral}} + \hat{\varepsilon}_{\text{qm}} \quad (\text{S11})$$

Written below are the results for each contribution up to the third order in ξ :

$$\hat{\varepsilon}_{\text{const}} = \begin{pmatrix} \varepsilon - \frac{g_{\perp}^2}{2\varepsilon} & ig_z & 0 \\ -ig_z & \varepsilon - \frac{g_{\perp}^2}{2\varepsilon} & 0 \\ 0 & 0 & \varepsilon \end{pmatrix} + \xi^2 \begin{pmatrix} \frac{q^2 g_{\perp}^4}{16b^2 \varepsilon^2} & 0 & 0 \\ 0 & \frac{q^2 g_{\perp}^4}{16b^2 \varepsilon^2} & 0 \\ 0 & 0 & \frac{q^2 g_{\perp}^2}{b^2} \end{pmatrix} \quad (\text{S12})$$

$$\hat{\varepsilon}_{\text{chiral}} = \xi \begin{pmatrix} 0 & 0 & -\frac{ig_{\perp}^2 k_y}{2b\varepsilon} \\ 0 & 0 & \frac{ig_{\perp}^2 k_x}{2b\varepsilon} \\ \frac{ig_{\perp}^2 k_y}{2b\varepsilon} & -\frac{ig_{\perp}^2 k_x}{2b\varepsilon} & 0 \end{pmatrix} + \xi^3 \frac{iq^2 g_{\perp}^2 k_y}{16b^3 \varepsilon^2} \begin{pmatrix} 0 & g_{\perp}^2 k_z & (g_{\perp}^2 - 8\varepsilon^2) k_y \\ -g_{\perp}^2 k_z & 0 & (g_{\perp}^2 - 8\varepsilon^2) k_x \\ -(g_{\perp}^2 - 8\varepsilon^2) k_y & -(g_{\perp}^2 - 8\varepsilon^2) k_x & 0 \end{pmatrix} \quad (\text{S13})$$

$$\hat{\varepsilon}_{\text{qm}} = \xi^3 \frac{q^2 g_{\perp}^2 g_z}{2b^3 \varepsilon} \begin{pmatrix} 0 & 0 & k_x \\ 0 & 0 & k_y \\ k_x & k_y & 0 \end{pmatrix} \quad (\text{S14})$$

Imaginary Hermitian matrix $\hat{\varepsilon}_{\text{chiral}}$ can be re-interpreted as electromagnetic chirality. Non-reciprocal term $\hat{\varepsilon}_{\text{qm}}$ characterizes spatial dispersion which cannot be described with bianisotropic parameters. The corresponding value χ_{qm} is found to be

$$\chi_{\text{qm}} = \frac{q^3 g_{\perp}^2 g_z}{2b^3 \varepsilon} = \frac{q^3 g^3}{2b^3 \varepsilon} \sin^2 \beta \cos \beta.$$

A similar result can be obtained when magnetic permeability is gyrotropic, i. e.

$$\mathbf{B} = \mathbf{H} - i[\mathbf{g} \times \mathbf{H}].$$

In this case the calculation for $\hat{\iota}_{\text{eff}}$ is carried out in a similar manner, and, again, the matrix $\hat{\iota}$ has a block-diagonal form, acquiring a spatially-dispersive contribution in some components. In this case we have nontrivial magnetic permeability:

$$\hat{\mu} = \hat{\mu}_{\text{const}} + \hat{\mu}_{\text{chiral}} + \hat{\mu}_{\text{qm}}, \quad (\text{S15})$$

$$\hat{\mu}_{\text{qm}} = -\xi^3 \frac{q^2 g_{\perp}^2 g_z}{2b^3 \varepsilon} \begin{pmatrix} 0 & 0 & k_x \\ 0 & 0 & k_y \\ k_x & k_y & 0 \end{pmatrix}. \quad (\text{S16})$$

Here the magnitude of spatial dispersion reads

$$\chi_{\text{qm}} = -\frac{q^3 g_{\perp}^2 g_z}{2b^3 \varepsilon} = -\frac{q^3 g^3}{2b^3 \varepsilon} \sin^2 \beta \cos \beta.$$

If the mapping to spatially-dispersive permittivity is applied, we obtain third-order corrections in \mathbf{k} :

$$\varepsilon(q, \mathbf{k}) = 1 + \frac{1}{q^2} \mathbf{k}^{\times} (\mu^{-1} - \hat{1}) \mathbf{k}^{\times}$$

Despite the difference in the effective permittivity, shown by this derivation, physically magnetic and electric quasi-moving dispersion result in the same optical phenomena and the duality transformation provides a map between them.

In the main text, we examine the implications of this nonreciprocal effect, applicable to both electric and magnetic-type quasi-moving dispersion.

III. ESTIMATES OF THE QUASI-MOVING EFFECT IN MICROWAVE METAMATERIALS

In this section, we estimate the magnitude of the quasi-moving spatial dispersion available in microwave metamaterials. For the estimates, we employ the parameters of Ref. [2] which studied photonic anti-chiral edge states in a microwave structure composed of magnetized YIG cylinders. The permeability of yttrium iron garnet (YIG) cylinders is approximated by

$$\hat{\mu} = \begin{pmatrix} \mu_r & -ig & 0 \\ ig & \mu_r & 0 \\ 0 & 0 & 1 \end{pmatrix},$$

where all parameters depend on the operating frequency ω as

$$\mu_r = 1 + \frac{\omega_0 + i\alpha\omega}{(\omega_0 + i\alpha\omega)^2 - \omega^2}, \quad g = 1 + \frac{\omega_0 + i\alpha\omega}{(\omega_0 + i\alpha\omega)^2 - \omega^2}.$$

The frequencies $\omega_0 = \gamma\mu_0 H_z$, $\omega_m = \gamma\mu_0 M_s$ in these dependencies are functions of external magnetic flux density $\mu_0 H_z = 0.043$ T and magnetic flux density from saturation magnetization $\mu_0 M_s = 0.00224$ T. γ denotes gyromagnetic ratio and $\alpha = 0.0088$ is the damping coefficient. This dependency peaks at $\text{Re } g = 1.5$ near the resonance $\omega^2 \approx \omega_0^2$. We apply the expression

$$\chi_{\text{qm}} = \frac{1}{2} \left(\frac{2\pi\omega a}{c} \right)^3 g^3 \sin^2 \beta \cos \beta$$

to a metamaterial with a period $a = 0.12$ m. At resonance, we obtain $2\pi\omega a/c \approx 0.5$, where metamaterial approximation has some problems, but remains more or less valid. The maximum with respect to the cone angle β is achieved when $\beta = \arcsin \sqrt{2/3}$, in this case $\sin^2 \beta \cos \beta = 2/(3\sqrt{3})$. With all this, we arrive to an estimate

$$\chi_{\text{qm}} \approx 0.2.$$

It should be stressed that this is just an order of magnitude estimate, and the effect can be enhanced further by properly optimizing the geometry. On the other hand, the effect can be partly suppressed due to losses. However, at microwaves the effect of Ohmic losses is well controllable.

IV. FOCAL LENGTH OF A LENS IN A QUASI-MOVING MEDIUM

In this section, we calculate the parameters of a thin lens-shaped cavity cut in the quasi-moving material. We first evaluate the refractive index using the equation (S1), which exhibits the expected nonreciprocity linear in χ_{qm} :

$$n(k_x) = \frac{\sqrt{k_x^2 + k_y^2}}{q} = \sqrt{\epsilon} + k_x^2 \left(\pm \frac{\chi_{\text{qm}}}{q^2 \epsilon} - \frac{\chi_{\text{qm}}^2}{2q^2 \epsilon^{3/2}} \right) + O(k_x^4). \quad (\text{S17})$$

To compute the focal distance of a thin lens, we utilize the second-order approximation for the dependency between the angle and the refractive index

$$n(\theta) = n_{\parallel} + \zeta \frac{k_x^2}{k_z^2} = n_{\parallel} + \zeta \sin^2 \theta \quad (\text{S18})$$

in the paraxial limit applying the geometric optics approximation. We assume that z is the optical axis, an object is located at $(x_o, 0, z_o)$, the light ray emitted by the object intersects the lens surface at the point $(x_1, y_1, z_1(x_1, y_1))$. The surface is spherical, given by the equation

$$z_1(x_1, y_1) = R_1 - \sqrt{R_1^2 - x_1^2 - y_1^2},$$

where R_1 denotes curvature radius. Series expansion for optical path length up to the terms quadratic in x_o , x_1 , y_1 reads

$$\Delta = -n_{\parallel} z_o + \frac{n_{\parallel} + 2\zeta}{z_o} x_o (x_1 - x_o/2) + \frac{n_{\parallel} (z_o/R_1 - 1) - 2\zeta}{2z_o} (x_1^2 + y_1^2). \quad (\text{S19})$$

The surface may separate a medium with parameters $n_{1\parallel}$, ζ_1 from another medium characterized by $n_{2\parallel}$, ζ_2 . In this case we find the location of image by equating coefficients in (S19), namely

$$\begin{cases} \frac{n_{1\parallel} + 2\zeta_1}{z_o} x_o = \frac{n_{2\parallel} + 2\zeta_2}{z_{i0}} x_{i0}, \\ \frac{n_{1\parallel} + 2\zeta_1}{z_o} - \frac{n_{1\parallel}}{R_1} = \frac{n_{2\parallel} + 2\zeta_2}{z_{i0}} - \frac{n_{2\parallel}}{R_1}, \end{cases} \quad (\text{S20})$$

where x_{i0} and z_{i0} are coordinates of the intermediate image. The lens boundary consists of the two surfaces, on the second surface the image of the intermediate image is cast. We consider a thin lens with $n_{1\parallel}$, ζ_1 embedded in the medium possessing $n_{2\parallel}$, ζ_2 . Applying Eq. (S20) twice we obtain

$$\begin{cases} \frac{n_{1\parallel} + 2\zeta_1}{z_o} x_o = \frac{n_{2\parallel} + 2\zeta_2}{z_{i0}} x_{i0} = \frac{n_{1\parallel} + 2\zeta_1}{z_i} x_i, \\ \frac{n_{1\parallel} + 2\zeta_1}{z_o} - \frac{n_{1\parallel}}{R_1} = \frac{n_{2\parallel} + 2\zeta_2}{z_{i0}} - \frac{n_{2\parallel}}{R_1}, \\ \frac{n_{2\parallel} + 2\zeta_2}{z_{i0}} - \frac{n_{2\parallel}}{R_2} = \frac{n_{1\parallel} + 2\zeta_1}{z_i} - \frac{n_{1\parallel}}{R_2}, \end{cases} \quad (\text{S21})$$

where x_i and z_i indicate the position of the final image, R_2 denotes the radius of the rightmost surface. From these equations we extract the thin lens formula as well as image magnification. The thin lens formula is similar to the case of a lens made with isotropic materials, but with a modified focal distance:

$$\frac{1}{z_i} - \frac{1}{z_o} = \frac{n_{2\parallel} - n_{1\parallel}}{n_{1\parallel} + 2\zeta} \left(\frac{1}{R_1} - \frac{1}{R_2} \right) \quad (\text{S22})$$

Magnification of a lens coincides exactly with the classical result. It equals the ratio between distances from the center of the lens to an object and its image:

$$\frac{x_i}{x_o} = \frac{z_i}{z_o} \quad (\text{S23})$$

The equation (S22) is used in the main text to showcase the effect of non-reciprocal lensing.

V. DIPOLE RADIATION IN A QUASI-MOVING MEDIUM

In this section we investigate the dipole radiation in a quasi-moving medium focusing on the asymmetry of the radiation pattern. We consider a point electric dipole \mathbf{d} oscillating with the frequency ω , corresponding to charge density and current

$$\rho = d \delta(x) \delta(y) \delta'(z), \quad \mathbf{j} = i\omega \mathbf{d} \delta(x) \delta(y) \delta(z).$$

We apply Fourier transformation to Maxwell's equations, obtaining

$$\begin{aligned} i\mathbf{k} \times \mathbf{B} + iq\mathbf{D} &= \frac{4\pi}{c} \frac{i\omega \mathbf{d}}{(2\pi)^3}, \\ i\mathbf{k} \times \mathbf{E} - iq\mathbf{B} &= 0. \end{aligned}$$

The amplitude of electric field is found by solving the linear system

$$\hat{M} \mathbf{E}(\mathbf{k}) = \frac{1}{2\pi^2} \mathbf{d}, \quad \hat{M} = \frac{\mathbf{k}^{\times 2}}{q^2} + \hat{\epsilon} = \frac{\mathbf{k} \otimes \mathbf{k} - k^2 \hat{1}}{q^2} + \hat{\epsilon}.$$

Inverse Fourier transformation yields

$$\mathbf{E}(\mathbf{r}) = \frac{1}{2\pi^2} \int d^3 \mathbf{k} e^{i\mathbf{kr}} \hat{M}^{-1} \mathbf{d}.$$

The matrix \hat{M} is singular at the isofrequency surface. We adjust the poles assuming the oscillations start adiabatically in the past and replace q with $q + i0$. If $\mathbf{k} = \mathbf{k}_{\parallel} + \mathbf{k}_{\perp}$, $\mathbf{k}_{\parallel} \parallel \mathbf{r}$ and $\mathbf{k}_{\perp} \perp \mathbf{r}$, then

$$\mathbf{E}(\mathbf{r}) = \int d^2\mathbf{k}_{\perp} \int dk_{\parallel} e^{ik_{\parallel}r} \frac{1}{\det \hat{M}} \text{adj}(\hat{M}) \frac{1}{2\pi^2} \mathbf{d} = \int d^2\mathbf{k}_{\perp} e^{ik_{\parallel i}r} 2\pi i \left(\underset{k_{\parallel}=k_{\parallel i}}{\text{res}} \frac{1}{\det \hat{M}} \right) \text{adj}(\hat{M}(k_{\parallel i})) \frac{1}{2\pi^2} \mathbf{d},$$

where $k_{\parallel i}(k_{\perp})$ is the wave-vector projection when the vector lies on the isofrequency surface, $\text{adj}(\hat{M})$ denotes the adjugate matrix to \hat{M} . This evaluation is only applicable when the rank of \hat{M} is 2 on the isofrequency surface, which is the case when $\chi_{qm} \neq 0$ and \mathbf{k} is not parallel to z axis. Higher degeneracies render this particular method inapplicable, but path integrals of the matrix elements of \hat{M}^{-1} may still be evaluated. Further analytical integration of the given expression is not viable in the general case, however far field calculations can be done using stationary phase approximation. Whenever r is large, the rapid oscillations of $e^{ik_{\parallel i}r}$ average out to zero, except for the vicinities of local extrema of $k_{\parallel i}$. For these points, the series expansion

$$k_{\parallel i} = k_{\parallel i 0} + \frac{1}{2} \left(\frac{\partial^2 k_{\parallel i}}{\partial k_{\perp 1}^2} k_{\perp 1}^2 + \frac{\partial^2 k_{\parallel i}}{\partial k_{\perp 2}^2} k_{\perp 2}^2 \right) + O(|\mathbf{k}_{\perp}|^3)$$

is used, where $k_{\perp 1}$ and $k_{\perp 2}$ are the coordinates of \mathbf{k}_{\perp} in an orthonormal basis diagonalizing the quadratic approximation of the dependency $k_{\parallel i}(\mathbf{k}_{\perp})$. Exponential functions of quadratic expressions are readily integrated using an analytical result

$$\int_{-\infty}^{\infty} e^{ibx^2/2} dx = \sqrt{\frac{2\pi i}{b}}.$$

Thus, we recover the final expression for the far-field amplitude:

$$\mathbf{E}(\mathbf{r}) = -\frac{2e^{ik_{\parallel}r}}{r} \left(\frac{\partial \det \hat{M}}{\partial k_{\parallel}} \right)^{-1} \left(\frac{\partial^2 k_{\parallel i}}{\partial k_{\perp 1}^2} \frac{\partial^2 k_{\parallel i}}{\partial k_{\perp 2}^2} \right)^{-1/2} \text{adj}(\hat{M}) \mathbf{d} \Bigg|_{k_{\perp}=0, k_{\parallel}=k_{\parallel i 0}}.$$

The second derivatives combine to the Gaussian curvature of the isofrequency surface, which we denote by K .

$$K = \frac{\partial^2 k_{\parallel i}}{\partial k_{\perp 1}^2} \frac{\partial^2 k_{\parallel i}}{\partial k_{\perp 2}^2}.$$

Both electric and magnetic fields can be computed, considering the Fourier image of \mathbf{H} reads $\mathbf{H}(\mathbf{k}) = -(\mathbf{k}^{\times}/q)\mathbf{E}(\mathbf{k})$.

$$\mathbf{E}(\mathbf{r}) = -\frac{2e^{ik_{\parallel}r}}{\sqrt{K}r} \left(\frac{\partial \det \hat{M}}{\partial k_{\parallel}} \right)^{-1} \text{adj}(\hat{M}) \mathbf{d} \Bigg|_{k_{\perp}=0, k_{\parallel}=k_{\parallel i 0}}, \quad (\text{S24})$$

$$\mathbf{H}(\mathbf{r}) = \frac{2e^{ik_{\parallel}r}}{\sqrt{K}r} \left(\frac{\partial \det \hat{M}}{\partial k_{\parallel}} \right)^{-1} \frac{\mathbf{k}^{\times}}{q} \text{adj}(\hat{M}) \mathbf{d} \Bigg|_{k_{\perp}=0, k_{\parallel}=k_{\parallel i 0}}. \quad (\text{S25})$$

These results are enough to find the Poynting vector, which acquires a spatial dispersion-induced correction in our case [3]

$$\mathbf{S} = \frac{c}{8\pi} \left(\text{Re} \mathbf{E}^* \times \mathbf{H} - \frac{q}{2} \frac{\partial \varepsilon_{ij}}{\partial \mathbf{k}} E_i^* E_j \right)$$

The angular distribution of radiation power can be of interest. We evaluate it as a Poynting vector flux through a section of a distant sphere

$$\frac{\delta P}{\delta \Omega_S} = \frac{r^2 \delta \Omega_r \mathbf{S} \cdot \mathbf{n}_r}{\delta \Omega_S},$$

where Ω_r and Ω_S are solid angles for position on the sphere and Poynting vector respectively, $\mathbf{n}_r = \mathbf{r}/r$. We write

$$\begin{aligned} \delta \Omega_S &= \sin \theta_S \delta \theta_S \delta \phi_S, \\ \delta \Omega_r &= \sin \theta_r \delta \theta_r \delta \phi_r, \end{aligned}$$

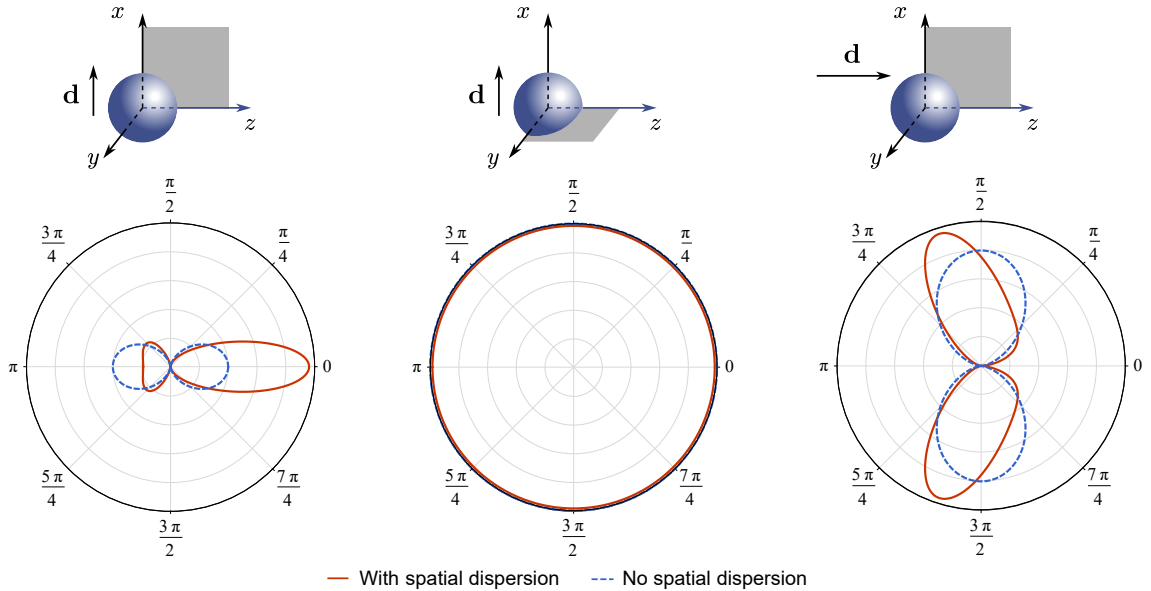


FIG. S1. Radiation patterns of a point dipole in the far field, depending on the dipole orientation, with the magnitude of non-reciprocity $\chi_{qm} = -0.2$.

arriving to the expression for the power distribution in terms of the Poynting vector and the Jacobian of the solid angle mapping

$$\frac{\delta P}{\delta \Omega_S} = r^2 \mathbf{S} \cdot \mathbf{n}_r \frac{\partial(\cos \theta_r, \phi_r)}{\partial(\cos \theta_S, \phi_S)}.$$

Evaluated distributions are presented in Figure S1. If dipole is oscillating along z , the rotational axis of the material, we observe backscattering suppression due to the nonreciprocity [Fig. S1, right]. The pattern is rotationally symmetric.

The dipole oriented orthogonally to the rotation axis has a more complex asymmetric radiation pattern [Fig. S1, left]. Two cross-sections are shown in the figure. In the plane (xz) the nonreciprocity is apparent, however the quasi-moving nonlocality does not affect the radiation power distribution in the (yz) plane. In turn, asymmetric radiation pattern of a dipole ensures that the backscattering can be reduced in the entire bulk of the medium.

Notably, the radiation diagram for the dipole perpendicular to the symmetry axis is discontinuous at the limit $\mathbf{k} \rightarrow (0, 0, q)^\top$ – hence the radiation power has different values near the axis z for the first two panels of the figure. This is caused by eigenmode degeneracy when $\mathbf{k} = (0, 0, q)^\top$. In the vicinity of this vector the degeneracy breaks in different ways, depending on the direction of the wave vector. For instance, if $k_x \neq 0$ and $k_y = 0$, the ordinary mode is polarized along the axis y , and the extraordinary mode is polarized along x ; the dipole excites the extraordinary mode, affected by spatial dispersion. The situation is opposite when $k_y \neq 0$ and $k_x = 0$, in this case the emission is accomplished via the unchanged ordinary mode. Because these radiation channels have very different efficiency, owing to the difference in the curvatures of the isofrequency surfaces, the power noticeably varies when the observation point rotates around z .

The effect of discontinuity in the radiation pattern is not unique to the description of quasi-moving dispersion, a similar discontinuity is predicted for uniaxial crystals [4] when the dipole is not parallel to the anisotropy axis. It is instructive to outline similarities between uniaxial crystals and the quasi-moving media in the formalism of scalar Green's functions, used in the paper. For that, we recast the matrix from Maxwell's equations in the form

$$\hat{M}^{-1} = \frac{q^2}{d_1(\mathbf{k})} \hat{1} + \frac{1}{d_1(\mathbf{k}) d_2(\mathbf{k})} (n_1(\mathbf{k}) \mathbf{e}_z \otimes \mathbf{e}_z + n_2(\mathbf{k}) \mathbf{k} \otimes \mathbf{k} + n_3(\mathbf{k}) [\mathbf{k} \otimes \mathbf{e}_z + \mathbf{e}_z \otimes \mathbf{k}]),$$

where

$$\begin{aligned} d_1(\mathbf{k}) &= q^2 - \mathbf{k}^2, \\ d_2(\mathbf{k}) &= q^3 - qk_z^3 - (k_x^2 + k_y^2)(q + q\chi_{\text{qm}}^2 + 2\chi_{\text{qm}}k_z), \\ n_1(\mathbf{k}) &= q^3\chi_{\text{qm}}(\chi_{\text{qm}}(k_x^2 + k_y^2) + k_z(2q + \chi_{\text{qm}}k_z)), \\ n_2(\mathbf{k}) &= q(q^2[\chi_{\text{qm}}^2 - 1] + k_x^2 + k_y^2 + 2q\chi k_z + k_z^2), \\ n_3(\mathbf{k}) &= q^2\chi_{\text{qm}}(k_z q \chi_{\text{qm}} - k_x^2 - k_y^2 + k_z^2 + q^2). \end{aligned}$$

The Fourier image of \hat{M}^{-1} is the dyadic Green's function, expressed as

$$\hat{G}^{\text{ee}}(\mathbf{r}) = q^2 g_1(\mathbf{r}) \hat{1} + \{\mathbf{e}_z \otimes \mathbf{e}_z n_1(-i\nabla) - \nabla \otimes \nabla n_2(-i\nabla) - i[\nabla \otimes \mathbf{e}_z + \mathbf{e}_z \otimes \nabla] n_3(-i\nabla)\} g_3(\mathbf{r})$$

via scalar Green's functions

$$g_1(\mathbf{r}) = \int d^3\mathbf{k} \frac{1}{d_1(\mathbf{k})} e^{i\mathbf{kr}}, \quad g_2(\mathbf{r}) = \int d^3\mathbf{k} \frac{1}{d_2(\mathbf{k})} e^{i\mathbf{kr}}, \quad g_3(\mathbf{r}) = \int d^3\mathbf{k} \frac{1}{d_1(\mathbf{k})d_2(\mathbf{k})} e^{i\mathbf{kr}} = (g_1 * g_2)(\mathbf{r})$$

Here the operation $*$ denotes convolution. The mixed derivatives $\partial_x \partial_y$ of the function g_3 are not continuous at $r_x = r_y = 0$ (this parts acquires contributions from the wave vectors near $(0, 0, q)^T$), and as a consequence the radiated field amplitude is discontinuous as well. This method would provide an analytical near-field solution, if the expression for g_3 was analytically integrable.

[1] V. M. Agranovich and V. Ginzburg, *Crystal Optics with Spatial Dispersion, and Excitons* (Springer Berlin Heidelberg, 1984).
[2] P. Zhou, G.-G. Liu, Y. Yang, Y.-H. Hu, S. Ma, H. Xue, Q. Wang, L. Deng, and B. Zhang, Observation of Photonic Antichiral Edge States, *Physical Review Letters* **125**, 263603 (2020).
[3] L. Landau and E. Lifshitz, *Electrodynamics of Continuous Media* (Pergamon Press, Oxford, 1984).
[4] A. Hayat and M. Faryad, On the radiation from a hertzian dipole of a finite length in the uniaxial dielectric medium, *OSA Continuum* **2**, 1411 (2019).